Biochimica et Biophysica Acta 1798 (2010) 415–421

Contents lists available at ScienceDirect

Biochimica et Biophysica Acta

journal homepage: www.elsevier.com/locate/bbamem

Extracellular Mg^{2+} regulates the tight junctional localization of claudin-16 mediated by ERK-dependent phosphorylation

Akira Ikari [a,*], Keishi Kinjo [a], Kosuke Atomi [a], Yohei Sasaki [a], Yasuhiro Yamazaki [a], Junko Sugatani [a,b]

[a] Department of Pharmaco-Biochemistry, School of Pharmaceutical Sciences, University of Shizuoka, 52-1 Yada, Suruga-ku, Shizuoka 422-8526, Japan
[b] Global Center of Excellence for Innovation in Human Health Sciences, School of Pharmaceutical Sciences, University of Shizuoka, 52-1 Yada, Suruga-ku, Shizuoka 422-8526, Japan

ARTICLE INFO

Article history:
Received 22 July 2009
Received in revised form 13 October 2009
Accepted 5 November 2009
Available online 13 November 2009

Keywords:
Claudin-16
ERK
Phosphorylation

ABSTRACT

Claudin-16 is involved in the paracellular reabsorption of Mg^{2+} in the thick ascending limb of Henle. Little is known about the mechanism regulating the tight junctional localization of claudin-16. Here, we examined the effect of Mg^{2+} deprivation on the distribution and function of claudin-16 using Madin-Darby canine kidney (MDCK) cells expressing FLAG-tagged claudin-16. Mg^{2+} deprivation inhibited the localization of claudin-16 at tight junctions, but did not affect the localization of other claudins. Re-addition of Mg^{2+} induced the tight junctional localization of claudin-16, which was inhibited by U0126, a MEK inhibitor. Transepithelial permeability to Mg^{2+} was also inhibited by U0126. The phosphorylation of ERK was reduced by Mg^{2+} deprivation, and recovered by re-addition of Mg^{2+}. These results suggest that the MEK/ERK-dependent phosphorylation of claudin-16 affects the tight junctional localization and function of claudin-16. Mg^{2+} deprivation decreased the phosphothreonine levels of claudin-16. The phosphothreonine levels of T225A and T233A claudin-16 were decreased in the presence of Mg^{2+} and these mutants were widely distributed in the plasma membrane. Furthermore, TER and transepithelial Mg^{2+} permeability were decreased in the mutants. We suggest that the tight junctional localization of claudin-16 requires a physiological Mg^{2+} concentration and the phosphorylation of threonine residues via a MEK/ERK-dependent pathway.

1. Introduction

The tight junction (TJ) is the most apical intercellular junction of the lateral membrane in epithelial and endothelial cells. The TJ barrier contains aqueous channels capable of discriminating charge and molecular size, and shows quite variable electrical resistance among different epithelia [1, 2]. The TJ comprises a complex of multiple integral membrane, scaffolding, and signaling proteins. So far, a number of integral membrane proteins associated with the TJ have been identified, including occludin [3] and claudins [4–6]. The integral membrane proteins may come into contact with ions and solutes as they permeate through the paracellular pathway. Scaffolding proteins such as ZO-1 and ZO-2 play important roles in recruiting claudins to the TJ [7,8].

Claudins consist of a family of at least 24 homologous isoforms sharing several essential features [4–6]. The kidney is composed of numerous nephrons, which have several segments. Each segment has a distinct pattern of expression of claudins and a distinct role in the reabsorption of ions, water and molecules. Most Mg^{2+} is reabsorbed via a paracellular pathway in the thick ascending limb of Henle (TAL) [9]. Familial hypomagnesemia with hypercalciuria and nephrocalcinosis (FHHNC) is characterized by progressive renal Mg^{2+} and Ca^{2+} wasting, resulting in impaired renal function and renal failure. FHHNC has been genetically linked to mutations in the genes of claudin-16 and claudin-19 [10,11]. Both claudin-16 and claudin-19 are expressed in the TAL [12]. Therefore, disruption of one or both of them may affect the reabsorption of Mg^{2+} in the TAL leading to hypomagnesemia.

The phosphorylation of several claudins is involved in recruitment to the TJ and maintenance of the barrier function. Thr203 of claudin-1 is phosphorylated by MAP kinase and subsequently integrated into the TJ [13]. The barrier function of the T203A mutant of claudin-1 is weaker than that of the WT. WNK4, a serine/threonine kinase with no K, phosphorylates Ser206 of claudin-7 and promotes paracellular permeability to Cl^- [14]. Furthermore, the D564A mutant of WNK4 phosphorylates claudin-1, -2, -3, and -4, and increases paracellular Cl^- permeability [15]. Ser195 of claudin-4 is phosphorylated by an atypical PKC and subsequently integrated into the TJ [16]. We recently found claudin-16 to be phosphorylated at Ser217 by PKA [17]. A S217A mutant of claudin-16 did not localized to the TJ and showed no permeability to Mg^{2+}. Thus, the sites of phosphorylation and the enzymes involved differ for each claudin.

In the present study, we examined the effect of depriving cells of Mg^{2+} on the tight junctional localization and function of claudin-16 using an *in vitro* model of the epithelium. In Madin-Darby canine kidney (MDCK) cells expressing FLAG-tagged claudin-16, Mg^{2+}

Abbreviations: H-89, *N*-[2-(*p*-bromocinnamylamino)ethyl]-5-isoquinolinesulfonamide dihydrochloride; MDCK, Madin-Darby canine kidney; PKA, protein kinase A; TAL, thick ascending limb of Henle; TER, transepithelial electrical resistance

* Corresponding author. Tel.: +81 54 264 5776; fax: +81 54 264 5773.
E-mail address: ikari@u-shizuoka-ken.ac.jp (A. Ikari).

0005-2736/$ – see front matter © 2009 Elsevier B.V. All rights reserved.
doi:10.1016/j.bbamem.2009.11.005

deprivation decreased p-ERK level and the phosphothreonine levels of claudin-16. U0126, a MEK inhibitor, also reduced the phosphothreonine levels of claudin-16. T225A and T233A mutants of claudin-16 were not phosphorylated in the presence of Mg^{2+} and widely distributed in the plasma membrane. These mutants did not increase transepithelial permeability to Mg^{2+}. We suggest that a physiological Mg^{2+} concentration is required for claudin-16′s phosphorylation and localization to the TJ.

2. Materials and methods

2.1. Materials

Rabbit anti-claudin-1, anti-claudin-2, anti-claudin-3, and anti-ZO-1, and mouse anti-claudin-4 antibodies were obtained from Zymed Laboratories (South San Francisco, CA, USA). Rabbit anti-FLAG, and mouse anti-FLAG, anti-phosphoserine, and anti-phosphothreonine antibodies were from Sigma-Aldrich (Saint Louis, MO, USA). Exacta-Cruz B and C were from Santa Cruz Biotechnology (Santa Cruz, CA). Lipofectamine 2000 was from Invitrogen (Carlsbad, CA). All other reagents were of the highest grade of purity available.

2.2. Plasmid cDNA constructs

Rat claudin-16 cDNA was amplified by reverse transcription-PCR as described previously [18] and subcloned into the pCMV-Tag2A vector. Then, the FLAG-tagged CLDN-16 cDNA was amplified by reverse transcription-PCR and subcloned into the pTRE2hyg vector (BD Biosciences Clontech, Mountain View, CA, USA). The T225A and T233A mutants of claudin-16 were generated using a QuickChange site-directed mutagenesis kit (Stratagene, La Jolla, CA). Sequencing was performed by Bio Matrix Research (Chiba, Japan).

2.3. Cell culture and transfection

The MDCK Tet-OFF cell line was obtained from BD Biosciences Clontech. Cells were grown in Dulbecco's modified Eagle's medium (DMEM, Sigma-Aldrich) supplemented with 5% fetal calf serum (FCS, HyClone, Logan, UT, USA), 0.07 mg/ml penicillin-G potassium, 0.14 mg/ml streptomycin sulfate, and 0.1 mg/ml G418 in a 5% CO_2 atmosphere at 37 °C. The cells expressing FLAG-tagged WT claudin-16 were generated as described previously. The T225A and T233A mutants were transfected into MDCK Tet-OFF cells using Lipofectamine 2000 as recommended by the manufacturer. Stable transfectants were maintained in the presence of 0.1 mg/ml hygromycin B. DMEM normally contains 1 mM $MgCl_2$. Medium without $MgCl_2$ was prepared according to the composition of DMEM as a nominally Mg^{2+}-free medium. Its other components were the same as those of DMEM. The effect of Mg^{2+} deprivation was examined using the nominally Mg^{2+}-free medium.

2.4. Preparation of a membrane fraction and immunoprecipitation

Confluent MDCK cells were scraped into cold PBS and precipitated by centrifugation. The cells were then lysed in a RIPA buffer containing 150 mM NaCl, 0.5 mM EDTA, 1% Triton X-100, 50 mM Tris–HCl (pH 8.0), a protease inhibitor cocktail (Sigma-Aldrich) and 1 mM phenylmethylsulfonyl fluoride and sonicated for 20 s. After centrifugation at 1000×*g* for 5 min, the supernatant was collected (cell lysate) and the cell lysate (500 μg) was incubated with the anti-FLAG antibody and ExactaCruz B or C at 4 °C for 16 h with gentle rocking. After centrifugation at 6000×*g* for 1 min, the pellet was washed three times with the RIPA buffer. The cell lysate and immunoprecipitate were solubilized in a sample buffer for SDS-polyacrylamide gel electrophoresis. Protein concentrations were measured using a protein assay kit (Bio-Rad Laboratories, Hercules, CA) with bovine serum albumin as the standard.

2.5. SDS-polyacrylamide gel electrophoresis and immunoblotting

SDS-polyacrylamide gel electrophoresis was carried out as described previously [19]. In brief, the cell lysate (30 μg) or immunoprecipitate was applied to the SDS-polyacrylamide gel. Proteins were blotted onto a PVDF membrane and incubated with each primary antibody followed by a peroxidase-conjugated secondary antibody. Finally, the blots were stained with an ECL Western blotting kit from GE Healthcare Bio-Science.

2.6. Measurement of paracellular permeability

MDCK cells expressing FLAG-tagged claudin-16 were plated at confluent densities on transwells with polyester membrane inserts (Corning Incorporated-Life Sciences, Acton, MA). TER was measured as described previously [18]. To measure paracellular permeability to FITC-dextran, FITC-dextran (4000 Da, 0.5 mg/ml) was applied to the apical or basal compartment. The buffer contained 140 mM NaCl, 5.8 mM KCl, 0.34 mM Na_2HPO_4, 0.44 mM KH_2PO_4, 1 mM $CaCl_2$, 1 mM $MgCl_2$, 25 mM glucose and 20 mM Hepes (pH 7.4). After 1 h, the buffer in the opposite compartment was collected and fluorescent intensity was measured with a Fluoroskan Ascent CF (Thermo Labosystems). The paracellular permeability to Mg^{2+} from the apical to basal or from the basal to apical compartment was measured using Xylidyl Blue-I (XB-I). At time 0, the buffer (140 mM NaCl, 5.8 mM KCl, 0.34 mM Na_2HPO_4, 0.44 mM KH_2PO_4, 1 mM $CaCl_2$, 25 mM glucose and 20 mM Hepes, pH 7.4) supplemented with 10 mM $MgCl_2$ was poured into the filter well or the outside compartment. The opposite compartment was filled with the buffer without $MgCl_2$. After incubation at 37 °C for 1 h, the opposite compartment's buffer was collected and subjected to Mg^{2+} measurements. XB-I formed a complex with an absorbance maximum of 520 nm upon binding Mg^{2+} under alkaline conditions and the absorbance was measured with a BioSpec-mini spectrophotometer (Shimadzu, Kyoto, Japan). The calibration curve was rectilinear from 0 to 200 nmol/ml.

2.7. Confocal microscopy

MDCK cells expressing FLAG-tagged claudin-16 were plated at confluent densities on glass cover slips or transwells with polyester membrane inserts. Immunofluorescence microscopy was performed as described previously [18]. Immunolabeled cells were visualized on an LSM 510 confocal microscope (Carl Zeiss, Germany) set with a filter appropriate for Alexa Fluor 488 (488 nm excitation, 530 nm emission) and Alexa Fluor 546 (543 nm excitation, 585–615 nm emission). Images were further processed using Adobe Photoshop (Adobe System, San Jose, CA).

2.8. Statistics

Results are presented as the mean ± S.E.M. Differences between groups were assessed with a one-way analysis of variance, and corrections for multiple comparisons were made using Tukey's multiple comparison test. Significant differences were assumed at $p<0.05$.

3. Results

3.1. Effect of Mg^{2+} deprivation on the expression and localization of endogenous tight junctional proteins

Claudin-1, -2, -3, and -4 and ZO-1 were expressed endogenously in MDCK cells (Fig. 1). The exogenous claudin-16 expression was confirmed with the anti-FLAG antibody. The levels of claudins and ZO-1 were unchanged by Mg^{2+} deprivation. Immunofluorescence microscopy showed that FLAG-tagged claudin-16 was expressed in the cell–cell border area concomitant with ZO-1 (Fig. 2). The *xz*-scan

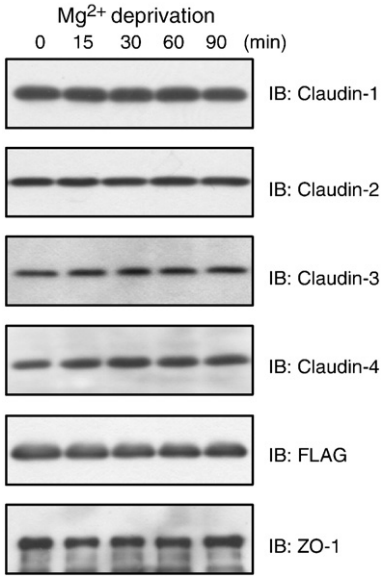

Fig. 1. Effect of Mg^{2+} deprivation on the expression of claudins and ZO-1. MDCK cells expressing FLAG-tagged claudin-16 were incubated in the absence of Mg^{2+} for the periods indicated. The cell lysates were separated by SDS-PAGE, and immunoblotted with anti-claudin-1, -2, -3, and -4, FLAG, and ZO-1 antibodies.

images revealed merged yellow spots near the most apical regions. Claudin-16 was distributed in the apical and lateral membranes. However, the distribution of ZO-1 was not affected by the deprivation. Re-addition of Mg^{2+} at 1 mM induced the localization of claudin-16 at the TJ, which was inhibited by U0126, a MEK inhibitor. These results indicate that a physiological Mg^{2+} concentration is necessary for claudin-16 to localize at the TJ. In contrast, the distribution of claudin-1, -2, -3, and -4, and ZO-1 was not affected by Mg^{2+} deprivation (Fig. 3). We next examined the effect of withholding Mg^{2+} from the apical or basal side on the localization of claudin-16. The distribution of claudin-16 was changed by withholding Mg^{2+} from the apical side, but not by withholding it from the basal side (Fig. 4). The distribution of claudin-16 was unchanged in the presence of more than 0.4 mM of Mg^{2+} on the apical side. However, claudin-16 was distributed in the apical and lateral membranes in the presence of less than 0.2 mM of

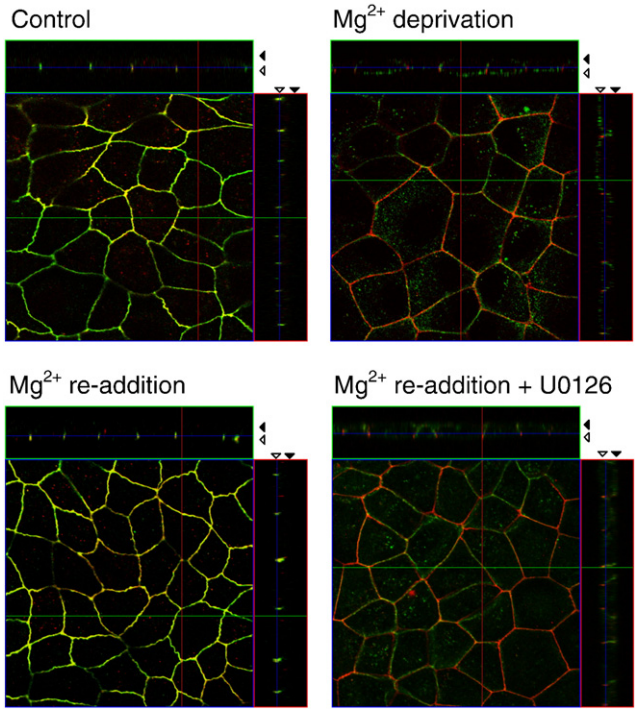

Fig. 2. Effect of extracellular Mg^{2+} and U0126 on the localization of FLAG-tagged claudin-16 at the TJ. The cells expressing FLAG-tagged claudin-16 were incubated in DMEM (control) or the nominally Mg^{2+}-free medium (Mg^{2+} deprivation) for 1 h. After Mg^{2+} deprivation, the cells were incubated in the presence of 1 mM $MgCl_2$ (Mg^{2+} re-addition) or 1 mM $MgCl_2$ plus 25 μM U0126 (Mg^{2+} re-addition + U0126) for 1 h. The cells were double stained with anti-FLAG (green) and anti-ZO-1 antibodies (red). The co-localization of the FLAG-tagged claudin-16 and ZO-1 appears yellow in the *x*–*y* image. Upper and right panels show the vertical sections (*x*–*z* image). Open and closed triangles represent apical and basal sides, respectively.

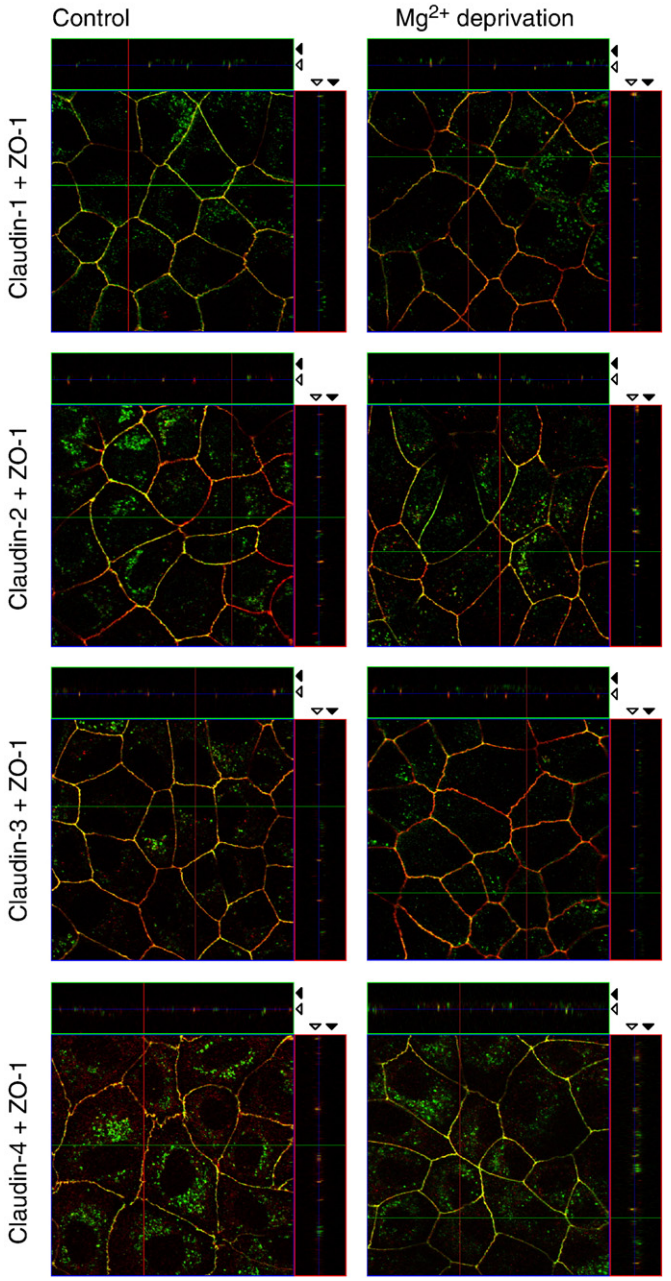

Fig. 3. Effect of Mg^{2+} deprivation on the localization of endogenous claudins at the TJ. The cells expressing FLAG-tagged claudin-16 were incubated in DMEM (control) or the nominally Mg^{2+}-free medium (Mg^{2+} deprivation) for 1 h. The cells were double stained with anti-ZO-1 (red) plus anti-claudin-1, -2, -3, or -4 antibodies (green). The co-localization of claudins and ZO-1 appeared yellow in the *x*–*y* image. Upper and right panels show the vertical sections (*x*–*z* image). Open and closed triangles represent apical and basal membrane, respectively.

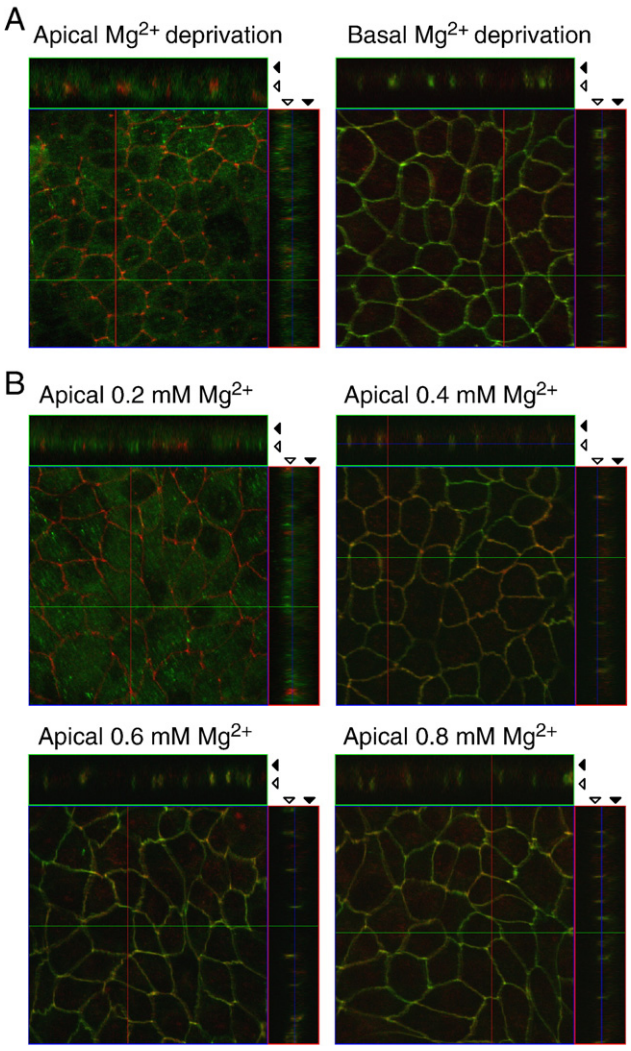

Fig. 4. Effect of Mg^{2+} deprivation in the apical or basal compartment on the localization of FLAG-tagged claudin-16. The cells expressing FLAG-tagged claudin-16 were cultured on transwell inserts. The cells were incubated for 1 h after the apical or basal medium was changed to nominally Mg^{2+}-free medium (A), or after the apical medium was changed to 0.2, 0.4, 0.6, or 0.8 mM $MgCl_2$-containing medium (B). The cells were double stained with anti-FLAG (green) and anti-ZO-1 (red) antibodies. The co-localization of the FLAG-tagged claudin-16 and ZO-1 appears yellow in the *x*–*y* image. Upper and right panels show the vertical sections (*x*–*z* image). Open and closed triangles represent the apical and basal sides, respectively.

Mg^{2+}. These results suggest that the localization of claudin-16 in the TJ is inhibited by a decrease in the Mg^{2+} concentration in the tubule lumen.

3.2. Dissociation of claudin-16 from ZO-1 on Mg^{2+} deprivation

The intracellular free Mg^{2+} concentration has been suggested to affect the regulation of p-ERK [20, 21]. Depriving cells of extracellular Mg^{2+} decreased p-ERK level, which recovered to the basal level on the re-addition of Mg^{2+} (Fig. 5A and B). Claudin-16 was associated with ZO-1 under the control conditions (Fig. 5C). Mg^{2+} deprivation decreased the association between claudin-16 and ZO-1. Re-addition of 1 mM Mg^{2+} increased this association in a time-dependent manner (Fig. 5D). The association between claudin-16 and ZO-1 was inhibited by U0126. These results suggest that extracellular Mg^{2+} affects p-ERK level and the association between claudin-16 and ZO-1 is enhanced by p-ERK.

3.3. Decrease in TER and transepithelial permeability to Mg^{2+} caused by Mg^{2+} deprivation and U0126

MDCK cells expressing FLAG-tagged claudin-16 were cultured at confluent densities on transwells with polyester membrane inserts. The removal of doxycycline from media induced the expression of FLAG-tagged claudin-16 (Fig. 6A). U0126 did not affect the expression of FLAG-tagged claudin-16. So far, we have reported that claudin-16 expression increases TER [18]. The inducible-expression of claudin-16 increased TER, which was inhibited by U0126 (Fig. 6B). Permeability to FITC-dextran was not affected by the inducible-expression of claudin-16 and U0126 (Fig. 6C and D), indicating no change in the paracellular flux of uncharged molecules. The transepithelial permeability to Mg^{2+} from the apical to basal compartment was increased by the removal of doxycycline, which was inhibited by U0126 (Fig. 6E). In contrast, that from the basal to apical compartment was unchanged by doxycycline and U0126 (Fig. 6F). These results suggest that the inducible-expression of claudin-16 affects TER and transepithelial permeability to Mg^{2+} from the apical to basal compartment, which are up-regulated by a MEK/ERK pathway.

3.4. Decrease in the phosphothreonine levels of claudin-16 caused by Mg^{2+} deprivation and U0126

The Ser217 of claudin-16 is phosphorylated in the presence of FCS and the phosphoserine level is decreased by H-89, an inhibitor of protein kinase A [17]. We examined the effect of Mg^{2+} deprivation on the phosphorylation of serine, threonine and tyrosine residues of claudin-16. The serine and threonine residues were phosphorylated in the presence of Mg^{2+} (Fig. 7A). In contrast, we did not detect the phosphorylation of tyrosine (data not shown). Depriving cells of extracellular Mg^{2+} decreased phosphothreonine levels without affecting phosphoserine levels. Re-addition of Mg^{2+} increased the phosphothreonine levels without affecting the phosphoserine levels

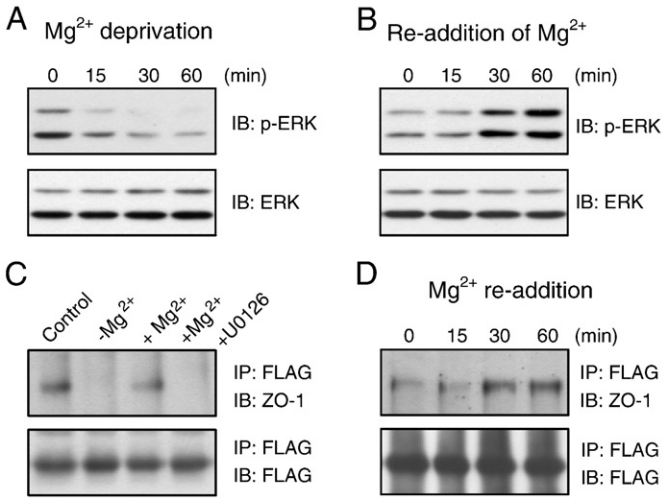

Fig. 5. Effect of extracellular Mg^{2+} on p-ERK and association between claudin-16 and ZO-1. (A and B) The cells expressing FLAG-tagged claudin-16 were incubated in the nominally Mg^{2+}-free medium (Mg^{2+} deprivation) for the periods indicated (A). After Mg^{2+} deprivation, the cells were incubated in the presence of 1 mM $MgCl_2$ for the periods indicated (B). The cell lysates were immunoblotted with anti-p-ERK and ERK antibodies. (C) The cells expressing FLAG-tagged claudin-16 were incubated in DMEM (control) or the nominally Mg^{2+}-free medium ($-Mg^{2+}$) for 1 h. After Mg^{2+} deprivation, the cells were incubated in the presence of 1 mM $MgCl_2$ ($+Mg^{2+}$) or 1 mM $MgCl_2$ plus 25 μM U0126 ($+Mg^{2+}$ + U0126) for 1 h. The cell lysates (500 μg) were immunoprecipitated with anti-FLAG antibody and the immune pellets were immunoblotted with anti-ZO-1 and anti-FLAG antibodies. (D) After Mg^{2+} deprivation, the cells were incubated in the presence of 1 mM $MgCl_2$ for the periods indicated. The cell lysates (500 μg) were immunoprecipitated with anti-FLAG antibody and the immune pellets were immunoblotted with anti-ZO-1 and anti-FLAG antibodies.

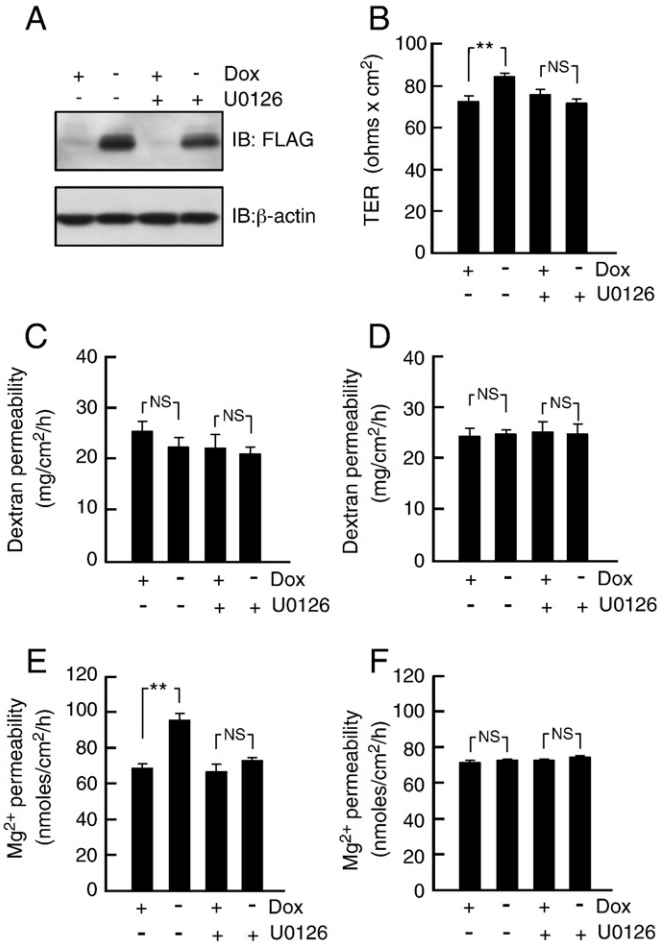

Fig. 6. Effect of U0126 on the expression and function of FLAG-tagged claudin-16. (A) The cells expressing FLAG-tagged claudin-16 were cultured for 3 days in the presence or absence of 100 ng/ml doxycycline. Then the cells were incubated with 25 μM U0126 for 1 h in the presence of Mg^{2+}. The cell lysates were immunoblotted with anti-FLAG and β-actin antibodies. (B) The cells were cultured on transwell inserts for 3 days in the presence or absence of 100 ng/ml doxycycline. Then the cells were incubated in the presence or absence of 25 μM U0126 for 1 h. TER was measured with a volt ohmmeter. (C and D) The FITC-dextran permeability from the apical to basal (C) or basal to apical (D) compartment was measured in cells incubated in the presence or absence of 25 μM U0126. FITC-dextran (4000 Da, 0.5 mg/ml) was applied to the apical compartment (C) or the basal compartment (D). After 1 h, the buffer in the opposite compartment was collected and fluorescent intensity was measured. (E and F) Transepithelial Mg^{2+} permeability from the apical to basal (E) or basal to apical (F) compartment was measured in cells incubated in the presence or absence of 25 μM U0126. The Mg^{2+} concentration was measured using XB-1. $^{**}P<0.01$ and ^{NS}, not significantly different.

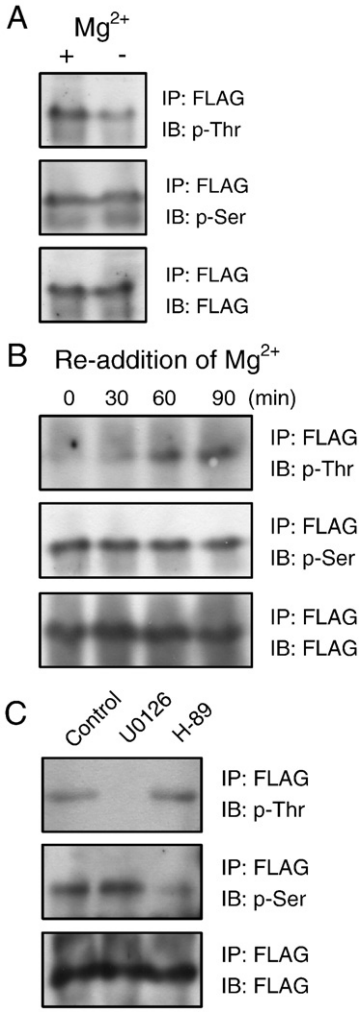

Fig. 7. Decrease in the phosphothreonine levels of claudin-16 caused by Mg^{2+} deprivation and U0126. (A) The cells expressing FLAG-tagged claudin-16 were incubated in DMEM (+) or the nominally Mg^{2+}-free medium (−) for 1 h. The cell lysates (500 μg) were immunoprecipitated with anti-FLAG antibody and the immune pellets were immunoblotted with anti-p-Thr, p-Ser and FLAG antibodies. (B) After Mg^{2+} deprivation for 1 h, the cells were incubated in the presence of 1 mM $MgCl_2$ for the periods indicated. The cell lysates were immunoprecipitated with anti-FLAG antibody and the immune pellets were immunoblotted with anti-p-Thr, p-Ser and FLAG antibodies. (C) The cells were incubated with 25 μM U0126 or 50 μM H-89 for 1 h. The cell lysates were immunoprecipitated with anti-FLAG antibody and the immune pellets were immunoblotted with anti-p-Thr, p-Ser and FLAG antibodies.

(Fig. 7B). The phosphorylation of threonine and serine residues of claudin-16 was decreased by U0126 and H-89, respectively (Fig. 7C). These results suggest the threonine residues of claudin-16 to be phosphorylated via a MEK/ERK pathway in the presence of Mg^{2+}.

3.5. Decrease in the phosphothreonine levels of claudin-16 and transepithelial permeability to Mg^{2+} caused by the mutation T225A or T233A

Claudin-16 contains four threonine residues in the cytoplasmic region, with those at 225 and 233 predicted to be phosphorylated according to the database on the NetPhos 2.0 Server (http://www.cbs.dtu.dk/services/NetPhos/). Therefore, we made FLAG-tagged claudin-16 mutants with T225A and T233A, and stably expressed them in the MDCK Tet-OFF cells. The expression of WT, T225A, and T233A claudin-16 was confirmed with the anti-FLAG antibody (Fig. 8A). WT claudin-16 was phosphorylated at threonine, but phosphothreonine levels were decreased in the mutants. Furthermore, the association with ZO-1 was decreased among T225A and T233A claudin-16. Immunofluorescence microscopy showed that the T225A and T233A mutants were widely distributed in the apical and lateral membranes (Fig. 8B). Levels of TER and transepithelial permeability to Mg^{2+} were lower in the T225A and T233A mutants than WT (Fig. 8C and D). These results suggest that the phosphorylation of claudin-16 at Thr225 and Thr233 is important for the protein's localization to the TJ.

4. Discussion

FHHNC is genetically linked to mutations of *claudin-16*, with over 40 mutations identified to date [22]. The mutations mainly occur in the extracellular loop and transmembrane domain. In the cytoplasmic region, only one mutation was identified by Muller et al. [23] and the patient showed severe but self-limiting childhood hypercalciuria with a preserved glomerular filtration rate. This mutation is T233R, located

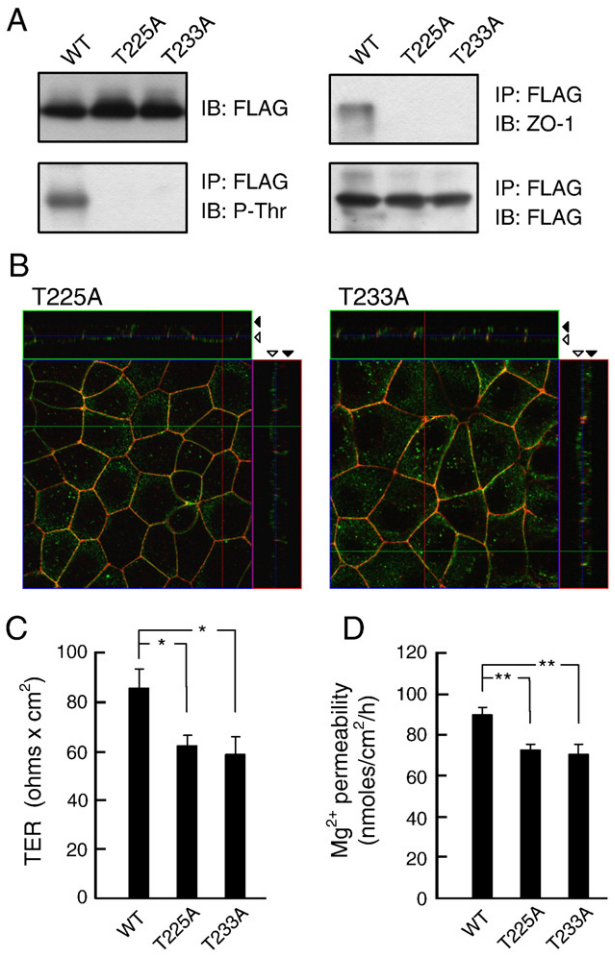

Fig. 8. Effect of the mutation T225A or T233A on the tight junctional localization and function of claudin-16. (A) Expression of the WT, T225A, or T233A mutant of FLAG-tagged claudin-16 was detected using anti-FLAG antibody. The cell lysates were immunoprecipitated with anti-FLAG antibody and the immune pellets were immunoblotted with anti-p-Thr, ZO-1 and FLAG antibodies. (B) The cells expressing the T225A or T233A mutant were double stained with anti-FLAG (green) and anti-ZO-1 (red) antibodies. Upper and right panels show the vertical sections (*x*–*z* image). The *x*–*z* images show that claudin-16 is widely distributed in the apical and lateral membranes, whereas ZO-1 is localized near the apical side. Open and closed triangles represent apical and basal sides, respectively. (C) TER was measured using the cells expressing WT, T225A, or T233A claudin-16. (D) Transepithelial Mg^{2+} permeability from the apical to basal compartment was measured using cells expressing WT, T225A, or T233A claudin-16. $^{**}P<0.01$ and $^{*}P<0.05$.

in the PDZ-binding motif of the carboxyl terminus. Claudins anchor to the TJ by binding to a scaffolding protein such as ZO-1, ZO-2, and ZO-3. The mutation of the PDZ-binding motif of claudin-16 inhibits the association with ZO-1, resulting in dissociation from the TJ [18,23,24].

Little is known about the non-genomic regulation of the localization of claudin-16 at the TJ. Our recent study showed that the phosphorylation of Ser217 by PKA is necessary for its localization at the TJ and dephosphorylated claudin-16 is translocated to the lysosome [17]. The mechanism of phosphorylation may play an important role in physiological and pathological conditions. Blood pressure is inversely associated with body Mg^{2+} levels [25] and dietary Mg^{2+} supplementation suppresses the development of hypertension [26]. The phosphoserine level of claudin-16 decreases in Dahl salt-sensitive hypertensive rats, suggesting Mg^{2+} reabsorption mediated via claudin-16 to be reduced in hypertensive rats [27]. Furthermore, the phosphoserine level of claudin-16 is reduced by high concentrations of extracellular divalent cations including Mg^{2+}, suggesting that the dissociation of claudin-16 from the TJ at high Mg^{2+} concentrations prevents excess reabsorption and backflow of Mg^{2+} from the peritubular space to tubule lumen [28]. In the present study, we found that Mg^{2+} deprivation and U0126 decreases p-ERK level and the phosphothreonine levels of claudin-16. Claudin-16 was dissociated from the TJ by the decrease in the phosphothreonine levels. The phosphoserine levels of claudin-16 were decreased by H-89, but not by Mg^{2+} deprivation and U0126 (Fig. 6). In contrast, the phosphothreonine levels of claudin-16 were decreased by Mg^{2+} deprivation and U0126, but not by H-89 (Figs. 4 and 6). The localization of claudin-16 may be dynamically regulated by both PKA- and ERK-dependent mechanisms. The reduction in the Mg^{2+} concentration in the apical compartment inhibited the tight junctional localization of claudin-16, whereas the reduction in the basal compartment did not. We suggest that the dissociation of claudin-16 from the TJ prevents backflow of Mg^{2+} from the peritubular space to tubule lumen when the Mg^{2+} concentration in the tubule is low.

Previously, we reported that claudin-16 increases TER and transepithelial permeability to Mg^{2+} in MDCK cells [17]. Claudin-16 decreases permeability to Na^{+} without affecting permeability to Cl^{-}, suggesting that TER is increased by the reduction in permeability to Na^{+}. The increases in TER and permeability to Mg^{2+} were correlated with the tight junctional localization of claudin-16 (Figs. 2, 6, and 8). In contrast, Hou et al. [29] reported that claudin-16 increases permeability to Na^{+} and Mg^{2+} in LLC-PK_1 cells. There is a discrepancy in that Na^{+} permeability is increased and decreased by claudin-16 expression in LLC-PK_1 and MDCK cells, respectively. Different effects on the permeability to Na^{+} of LLC-PK_1 and MDCK cells are observed with claudin-2 and -15 [30]. The permeability to Na^{+} and Cl^{-} differs in MDCK and LLC-PK_1 cells [31], and is determined by the combination of claudins. MDCK cells express claudin-1–4 and -7 [31], whereas LLC-PK_1 cells express claudin-1, -3, -4, and -7 [32]. Claudin-2 expression selectively increases permeability to cations. The difference in claudin-2 expression may affect permeability to Na^{+} and Cl^{-}. We suggest that claudin-16 expression had different effects on permeability to Na^{+} in MDCK and LLC-PK_1 cells because these cells have different combinations of claudin-16 and endogenous claudins.

In various nephron segments, Mg^{2+} reabsorption is modulated by many factors including hormones, Mg^{2+} restriction, Mg^{2+} load, and acid–base change [9]. In the TAL, paracellular Mg^{2+} reabsorption is increased by parathyroid hormone, Mg^{2+} restriction, and so on [33,34]. Unexpectedly, our data showed that Mg^{2+} deprivation decreases the phosphothreonine levels and the localization of claudin-16 at the TJ. The phosphothreonine levels of claudin-16 and transepithelial permeability to Mg^{2+} were decreased by U0126, suggesting that p-ERK is involved in the regulation of Mg^{2+} reabsorption. There is a possibility that the tight junctional localization and function of claudin-16 are indirectly regulated by peptide hormones in rats with Mg^{2+}-restricted diets. The ability to conserve Mg^{2+} is impaired in thyroparathyroidectomized rats on an Mg^{2+}-deficient diet. Parathyroid hormone increases p-ERK level in renal tubular cells [35,36]. We suggest that the phosphothreonine level and the localization of claudin-16 in the TJ are decreased in rats with Mg^{2+}-restricted diets, but increased by hormones such as parathyroid hormone in order to compensate for the reabsorption of Mg^{2+} in the TAL.

Claudin-16 was phosphorylated at different sites by two distinct kinases, PKA and ERK. The inhibition of each signaling pathway induced the dissociation of claudin-16 from the TJ and decrease in transepithelial permeability to Mg^{2+}. Claudin-16 is distributed in the lysosome or plasma membrane on a decrease in the phosphorylation of serine or threonine residues, respectively. We speculate that phosphoserine is involved in the trafficking of claudin-16 and phosphothreonine is involved in the anchoring to the TJ. Thr233 exists in the PDZ-binding motif of claudin-16. The localization and the interaction with PDZ-binding proteins of junctional adhesion molecules [37], multidrug resistance protein 2 [38], Kir4.1 K^{+} channels [39], and NMDA receptors [40] are affected by phosphorylation in the

PDZ-binding motif. Furthermore, it has been proposed that additional residues upstream of the PDZ-binding motif are also involved in binding PDZ protein [41]. The mutant with T225A, located −10 from the carboxyl terminus, was distributed in the plasma membrane and dissociated from ZO-1. We suggest that the phosphorylation of Thr225 also affects the interaction between the PDZ-binding motif of claudin-16 and ZO-1.

Taken together, claudin-16 is phosphorylated at Thr225 and Thr233 by a MEK/ERK-dependent pathway in this *in vitro* model of the epithelium. Mg^{2+} deprivation decreases p-ERK level, resulting in a decrease in the phosphothreonine levels of claudin-16. The decrease in phosphothreonine induced the dissociation of claudin-16 from the TJ and decrease in transepithelial permeability to Mg^{2+}. Reabsorption of Mg^{2+} in the TAL may be dynamically regulated by the phosphorylation of claudin-16.

Acknowledgements

This work was supported in part by the Ministry of Education, Science, Sports, and Culture of Japan, a Grant-in-Aid for Encouragement of Young Scientists (to A.I.), and by grants from the Salt Science Research Foundation (No. 0830), Mochida Memorial Foundation for Medical and Pharmaceutical Research, and the Research Foundation for Pharmaceutical Sciences (to A.I.).

References

[1] D.W. Powell, Barrier function of epithelia, Am. J. Physiol. 241 (1981) G275–G288.
[2] J.M. Anderson, C.M. Van Itallie, A.S. Fanning, Setting up a selective barrier at the apical junction complex, Curr. Opin. Cell Biol. 16 (2004) 140–145.
[3] M. Furuse, T. Hirase, M. Itoh, A. Nagafuchi, S. Yonemura, S. Tsukita, Occludin: a novel integral membrane protein localizing at tight junctions, J. Cell Biol. 123 (1993) 1777–1788.
[4] M. Furuse, K. Fujita, T. Hiiragi, K. Fujimoto, S. Tsukita, Claudin-1 and -2: novel integral membrane proteins localizing at tight junctions with no sequence similarity to occludin, J. Cell Biol. 141 (1998) 1539–1550.
[5] K. Morita, M. Furuse, K. Fujimoto, S. Tsukita, Claudin multigene family encoding four-transmembrane domain protein components of tight junction strands, Proc. Natl. Acad. Sci. U. S. A. 96 (1999) 511–516.
[6] S. Tsukita, M. Furuse, M. Itoh, Multifunctional strands in tight junctions, Nat. Rev. Mol. Cell Biol. 2 (2001) 285–293.
[7] A.S. Fanning, J.M. Anderson, Zonula occludens-1 and -2 are cytosolic scaffolds that regulate the assembly of cellular junctions, Ann. N. Y. Acad. Sci. 1165 (2009) 113–120.
[8] S. Tsukita, T. Katsuno, Y. Yamazaki, K. Umeda, A. Tamura, Roles of ZO-1 and ZO-2 in establishment of the belt-like adherens and tight junctions with paracellular permselective barrier function, Ann. N. Y. Acad. Sci. 1165 (2009) 44–52.
[9] G.A. Quamme, C. de Rouffignac, Epithelial magnesium transport and regulation by the kidney, Front. Biosci. 5 (2000) D694–D711.
[10] D.B. Simon, Y. Lu, K.A. Choate, H. Velazquez, E. Al-Sabban, M. Praga, G. Casari, A. Bettinelli, G. Colussi, J. Rodriguez-Soriano, D. McCredie, D. Milford, S. Sanjad, R.P. Lifton, Paracellin-1, a renal tight junction protein required for paracellular Mg^{2+} resorption, Science 285 (1999) 103–106.
[11] M. Konrad, A. Schaller, D. Seelow, A.V. Pandey, S. Waldegger, A. Lesslauer, H. Vitzthum, Y. Suzuki, J.M. Luk, C. Becker, K.P. Schlingmann, M. Schmid, J. Rodriguez-Soriano, G. Ariceta, F. Cano, R. Enriquez, H. Juppner, S.A. Bakkaloglu, M.A. Hediger, S. Gallati, S.C. Neuhauss, P. Nurnberg, S. Weber, Mutations in the tight-junction gene claudin 19 (CLDN19) are associated with renal magnesium wasting, renal failure, and severe ocular involvement, Am. J. Hum. Genet. 79 (2006) 949–957.
[12] S. Angelow, R. El-Husseini, S.A. Kanzawa, A.S. Yu, Renal localization and function of the tight junction protein, claudin-19, Am. J. Physiol. Renal Physiol. 293 (2007) F166–F177.
[13] M. Fujibe, H. Chiba, T. Kojima, T. Soma, T. Wada, T. Yamashita, N. Sawada, Thr203 of claudin-1, a putative phosphorylation site for MAP kinase, is required to promote the barrier function of tight junctions, Exp. Cell Res. 295 (2004) 36–47.
[14] R. Tatum, Y. Zhang, Q. Lu, K. Kim, B.G. Jeansonne, Y.H. Chen, WNK4 phosphorylates ser(206) of claudin-7 and promotes paracellular Cl^- permeability, FEBS Lett. 581 (2007) 3887–3891.
[15] K. Yamauchi, T. Rai, K. Kobayashi, E. Sohara, T. Suzuki, T. Itoh, S. Suda, A. Hayama, S. Sasaki, S. Uchida, Disease-causing mutant WNK4 increases paracellular chloride permeability and phosphorylates claudins, Proc. Natl. Acad. Sci. U. S. A. 101 (2004) 4690–4694.
[16] S. Aono, Y. Hirai, Phosphorylation of claudin-4 is required for tight junction formation in a human keratinocyte cell line, Exp. Cell Res. 314 (2008) 3326–3339.
[17] A. Ikari, S. Matsumoto, H. Harada, K. Takagi, H. Hayashi, Y. Suzuki, M. Degawa, M. Miwa, Phosphorylation of paracellin-1 at Ser217 by protein kinase A is essential for localization in tight junctions, J. Cell Sci. 119 (2006) 1781–1789.
[18] A. Ikari, N. Hirai, M. Shiroma, H. Harada, H. Sakai, H. Hayashi, Y. Suzuki, M. Degawa, K. Takagi, Association of paracellin-1 with ZO-1 augments the reabsorption of divalent cations in renal epithelial cells, J. Biol. Chem. 279 (2004) 54826–54832.
[19] A. Ikari, K. Nakajima, K. Kawano, Y. Suketa, Polyvalent cation-sensing mechanism increased Na^+-independent Mg^{2+} transport in renal epithelial cells, Biochem. Biophys. Res. Commun. 287 (2001) 671–674.
[20] R.M. Touyz, G. Yao, Modulation of vascular smooth muscle cell growth by magnesium—role of mitogen-activated protein kinases, J. Cell. Physiol. 197 (2003) 326–335.
[21] W.F. Waas, K.N. Dalby, Physiological concentrations of divalent magnesium ion activate the serine/threonine specific protein kinase ERK2, Biochemistry (Mosc.) 42 (2003) 2960–2970.
[22] D. Gunzel, L. Haisch, S. Pfaffenbach, S.M. Krug, S. Milatz, S. Amasheh, W. Hunziker, D. Muller, Claudin function in the thick ascending limb of Henle's loop, Ann. N. Y. Acad. Sci. 1165 (2009) 152–162.
[23] D. Muller, P.J. Kausalya, F. Claverie-Martin, I.C. Meij, P. Eggert, V. Garcia-Nieto, W. Hunziker, A novel claudin 16 mutation associated with childhood hypercalciuria abolishes binding to ZO-1 and results in lysosomal mistargeting, Am. J. Hum. Genet. 73 (2003) 1293–1301.
[24] P.J. Kausalya, S. Amasheh, D. Günzel, H. Wurps, D.M ü ller, M. Fromm, W. Hunziker, Disease-associated mutations affect intracellular traffic and paracellular Mg^{2+} transport function of Claudin-16, J. Clin. Invest. 116 (2006) 878–891.
[25] P.K. Whelton, M.J. Klag, Magnesium and blood pressure: review of the epidemiologic and clinical trial experience, Am. J. Cardiol. 63 (1989) 26G–30G.
[26] R.M. Touyz, F.J. Milne, Magnesium supplementation attenuates, but does not prevent, development of hypertension in spontaneously hypertensive rats, Am. J. Hypertens. 12 (1999) 757–765.
[27] A. Ikari, S. Matsumoto, H. Harada, K. Takagi, M. Degawa, T. Takahashi, J. Sugatani, M. Miwa, Dysfunction of paracellin-1 by dephosphorylation in Dahl salt-sensitive hypertensive rats, J. Physiol. Sci. 56 (2006) 379–383.
[28] A. Ikari, C. Okude, H. Sawada, Y. Sasaki, Y. Yamazaki, J. Sugatani, M. Degawa, M. Miwa, Activation of a polyvalent cation-sensing receptor decreases magnesium transport via claudin-16, Biochim. Biophys. Acta 1778 (2008) 283–290.
[29] J. Hou, D.L. Paul, D.A. Goodenough, Paracellin-1 and the modulation of ion selectivity of tight junctions, J. Cell Sci. 118 (2005) 5109–5118.
[30] C.M. Van Itallie, A.S. Fanning, J.M. Anderson, Reversal of charge selectivity in cation or anion-selective epithelial lines by expression of different claudins, Am. J. Physiol. Renal Physiol. 285 (2003) F1078–F1084.
[31] J. Hou, A.S. Gomes, D.L. Paul, D.A. Goodenough, Study of claudin function by RNA interference, J. Biol. Chem. 281 (2006) 36117–36123.
[32] M.D. Alexandre, Q. Lu, Y.H. Chen, Overexpression of claudin-7 decreases the paracellular Cl^- conductance and increases the paracellular Na^+ conductance in LLC-PK1 cells, J. Cell Sci. 118 (2005) 2683–2693.
[33] A. Di Stefano, M. Wittner, R. Nitschke, R. Braitsch, R. Greger, C. Bailly, C. Amiel, N. Roinel, C. de Rouffignac, Effects of parathyroid hormone and calcitonin on Na^+, Cl^-, K^+, Mg^{2+} and Ca^{2+} transport in cortical and medullary thick ascending limbs of mouse kidney, Pflugers Arch. 417 (1990) 161–167.
[34] A. Di Stefano, M. Wittner, R. Nitschke, R. Braitsch, R. Greger, C. Bailly, C. Amiel, J.M. Elalouf, N. Roinel, C. de Rouffignac, Effects of glucagon on Na^+, Cl^-, K^+, Mg^{2+} and Ca^{2+} transports in cortical and medullary thick ascending limbs of mouse kidney, Pflugers Arch. 414 (1989) 640–646.
[35] W.B. Sneddon, Y. Yang, J. Ba, L.M. Harinstein, P.A. Friedman, Extracellular signal-regulated kinase activation by parathyroid hormone in distal tubule cells, Am. J. Physiol. Renal Physiol. 292 (2007) F1028–F1034.
[36] S.J. Khundmiri, A.M. Bertorello, N.A. Delamere, E.D. Lederer, Clathrin-mediated endocytosis of Na^+,K^+-ATPase in response to parathyroid hormone requires ERK-dependent phosphorylation of Ser-11 within the alpha1-subunit, J. Biol. Chem. 279 (2004) 17418–17427.
[37] L.T. Braiterman, S. Heffernan, L. Nyasae, D. Johns, A.P. See, R. Yutzy, A. McNickle, M. Herman, A. Sharma, U.P. Naik, A.L. Hubbard, JAM-A is both essential and inhibitory to development of hepatic polarity in WIF-B cells, Am. J. Physiol. Gastrointest. Liver Physiol. 294 (2008) G576–G588.
[38] T. Hegedus, T. Sessler, R. Scott, W. Thelin, E. Bakos, A. Varadi, K. Szabo, L. Homolya, S.L. Milgram, B. Sarkadi, C-terminal phosphorylation of MRP2 modulates its interaction with PDZ proteins, Biochem. Biophys. Res. Commun. 302 (2003) 454–461.
[39] M. Tanemoto, T. Toyohara, T. Abe, S. Ito, MAGI-1a functions as a scaffolding protein for the distal renal tubular basolateral K+ channels, J. Biol. Chem. 283 (2008) 12241–12247.
[40] Y. Lin, T. Jover-Mengual, J. Wong, M.V. Bennett, R.S. Zukin, PSD-95 and PKC converge in regulating NMDA receptor trafficking and gating, Proc. Natl. Acad. Sci. U. S. A. 103 (2006) 19902–19907.
[41] Z. Songyang, A.S. Fanning, C. Fu, J. Xu, S.M. Marfatia, A.H. Chishti, A. Crompton, A.C. Chan, J.M. Anderson, L.C. Cantley, Recognition of unique carboxyl-terminal motifs by distinct PDZ domains, Science 275 (1997) 73–77.